Supplemental Material: Constrains on the order parameters of $CeRh_2As_2$ derived form low temperature ultrasonic spectroscopy.

S. Galeski[1,2,3,4†*], C. Lee[5 †], F. Bärtl[3, 8], J. Sourd[3], S. Zherlitsyn[3], A.T.M. Breugelmans[1], R. Amdouni[1], P. Khanenko[3, 6], E. Hassinger[6,7], S. Khim[6], J. Wosnitza[3,8], P. Thalmeier[6], P. M. R. Brydon[5], and M. Brando[6,]**

[1]HFML-FELIX, Toernooiveld 7, 6525ED Nijmegen, the Netherlands
[2]Institute for Molecules and Materials, Radboud University, Heyendaalseweg 135, 6525 AJ Nijmegen, The Netherlands
[3]Hochfeld-Magnetlabor Dresden (HLD-EMFL) and Würzburg-Dresden Cluster of Excellence ctd.qmat, Helmholtz-Zentrum Dresden-Rossendorf, 01328 Dresden, Germany
[4]Physikalisches Institut, Universität Bonn, Nussallee 12,53115 Bonn, Germany
[5]Department of Physics and MacDiarmid Institute for Advanced Materials and Nanotechnology, University of Otago, Dunedin, New Zealand
[6]Max Planck Institute for Chemical Physics of Solids, Nöthnitzer Straße 40, 01187 Dresden, Germany
[7]Institute for Quantum Materials and Technologies, Karlsruhe Institute of Technology, Kaiserstraße 12, 76131 Karlsruhe, Germany
[8]Technical University Dresden, Institute for Solid State and Materials Physics, 01062 Dresden, Germany
[†]contributed equally
[*]sgaleski@science.ru.nl
[**]brando@cpfs.mpg.de

ABSTRACT

This Supplemental Material provides additional experimental data and theoretical analysis supporting the main manuscript on the superconducting and magnetic order parameters in $CeRh_2As_2$. We present extended ultrasound measurements of elastic constants under applied magnetic fields and hydrostatic pressure. Furthermore, we develop a symmetry-based phenomenological Landau analysis of magnetoelastic coupling for magnetic ordering vectors at high-symmetry and generic points in the Brillouin zone. The conditions under which discontinuous jumps of elastic constants are permitted at the magnetic and superconducting transitions are derived and systematically classified.

Contents

1 Renormalization of the speed of sound under magnetic fields

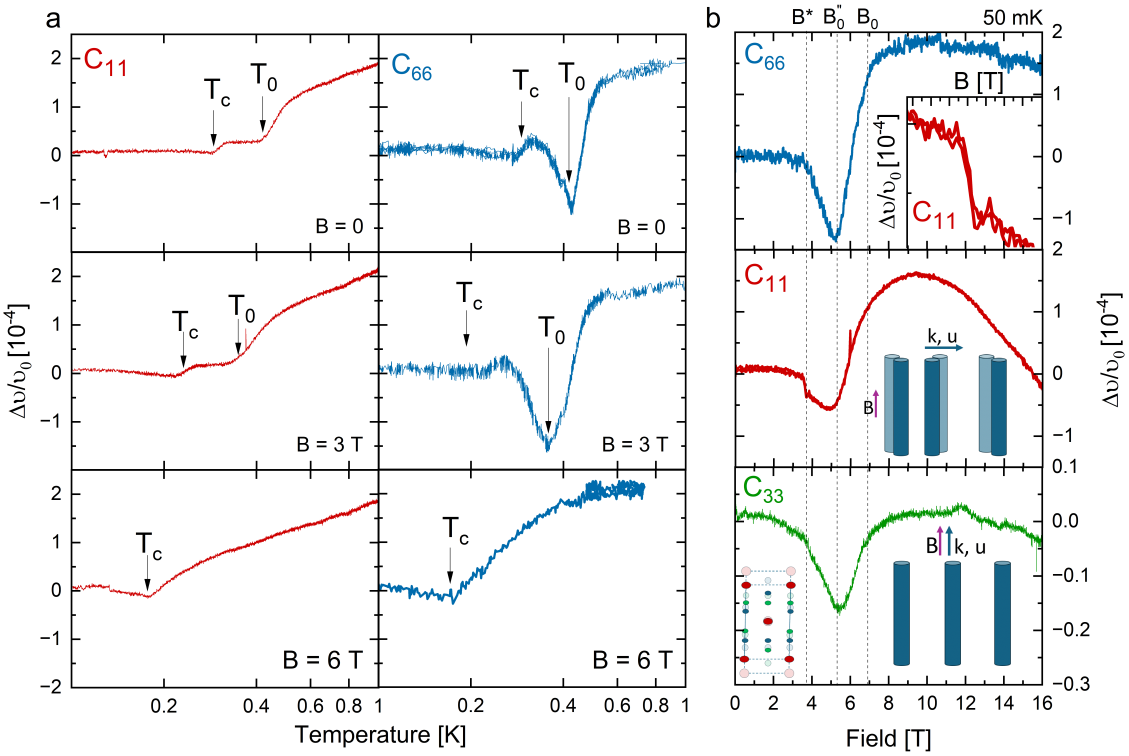

Figure S1. Influence of magnetic fields on the low-temperature elastic properties of $CeRh_2As_2$ a) Temperature dependence of the speed of sound reflecting the elastic modes C_{11} and C_{66} at selected magnetic fields. Application of magnetic fields leads to a decrease of the discontinuity in the elastic constants originating from the superconducting transition. b) Field dependence of the speed of sound of the elastic modes C_{11}, C_{66} and C_{33} elastic modes measured at 50 mK. Inset of the top panel is a zoom-in of the discontinuity seen in the field dependence of the C_{11} mode. Graphics in the middle and bottom panels schematically represent the interaction of compression weaves traveling parallel and perpendicular to the superconducting vortices, highlighting the insensitivity of the C_{33} elastic mode to vortex physics for $B \parallel c$.

Supplemental Material: Constrains on the order parameters of $CeRh_2As_2$ derived form low temperature ultrasonic spectroscopy.

Additional information about the nature of the superconducting phases of $CeRh_2As_2$ can be obtained by measurements in a magnetic field aligned with the crystallographic c axis as summarized in Fig. S1. Figure S1a shows the temperature dependence of the modes C_{11} and C_{66} with increasing magnetic fields. The shift of the anomalies in both elastic constants identified at zero field is consistent with the previously reported lowering of critical temperatures T_0 and T_c with the increasing out-of-plane magnetic field[1]. This evidences that the anomalies are due to the emergence of the magnetic and superconducting orders. The suppression of the height of the discontinuity at T_c can be tentatively interpreted as a decrease of the superconducting volume fraction of the material with the increase of flux lines penetrating the bulk, or as emerging due to the suppression of the coupling between the order parameter of phase I and the SC order parameter.

The field dependence of the elastic modes at the lowest temperature $T = 50\,\mathrm{mK}$ is presented in Fig. S1b. Here, the elastic modes remain almost constant in the SC-I phase until a slight softening occurs before crossing the proposed even-to-odd parity transition field at $B^* = 4\,\mathrm{T}$. Interestingly, due to the exceptional quality of the C_{11} data, a discontinuity in the C_{11} modulus is seen on crossing the transition. However, despite having the appearance of a first-order transition there is no observable hysteresis between up/down fields sweeps. This agrees with recent thermodynamic measurements performed across this transition[2]. In the other modes measured in magnetic fields, C_{33} and C_{66}, the parity transition is visible as a sharp change of slope without signatures of a discontinuity. At higher fields the transition across B_0 - which in the new samples was at about 7 T (cf. Fig. S1b)[2] - is visible in C_{66} and C_{33} as a broad step starting with a kink at about 5 T and ending at about 7 T. In C_{11} the saturation is not present, but a broad maximum appears at about 10 T. The reason for this behavior is unclear.

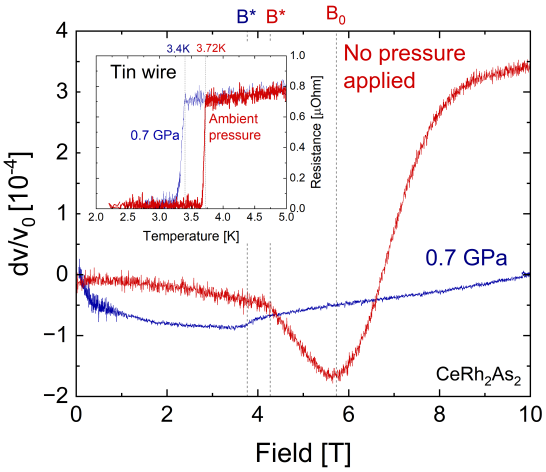

Figure S2. Field dependence of the elastic mode C_{66} measured in the pressure cell with and without applied pressure. Under pressure, signatures related to phase I are absent. However, the transition between the two SC phases remains visible. The inset shows the pressure-induced shift of T_c seen in the resistance of a tin wire used as a pressure gauge.

2 Additional measurements under pressure

To elucidate the nature of the order parameter in phase SC1, without the symmetry breaking induced by phase I, we have performed additional ultrasound experiment under pressure. In these measurements we measured the elastic constants C_{66} and C_{11} under pressure of $\simeq$0.7 GPa. In addition, for comparison with measurements under ambient conditions, we measured C_{66} in the pressure cell without loading any pressure. Comparison between the no-pressure and 0.7 GPa measurements of the C_{66} mode are shown in Figs.S2 and S3. Here, the control measurements in the pressure cell without applied pressure are in qualitative agreement with previous measurements done under ambient pressure presented in the main manuscript. Measurements under pressure revealed qualitatively new features. At 0.7 GPa, phase I is expected to be fully suppressed. Indeed, in the field dependence of C_{66} (Fig. S2) only a weak feature related to the transition between the superconducting phases of different parity is visible. Interestingly, in the temperature dependence (Fig. S3) no anomalies are detected, corroborating the scenario of a singe component SC OP.

In addition to C_{66} we have performed additional measurements of C_{11} to confirm effects of pressure on the speed of sound (Fig.S4 and Fig.S5). Here, similar to the case of C_{66}, only signatures of the parity transition are detected in the field sweep. Interestingly, despite the absence of phase I a stiffening of C_{11} is present at high fields in the SC2 phase (similarly to C_{66}) suggesting its relation to superconductivity. Furthermore, the temperature dependence reveals no signatures of phase I and a slight change of the slope close to ambient T_c, in agreement with the known $P-T$ phase diagram[3].

3 Magnetic order parameters at Cerium atom sites in $CeRh_2As_2$ and associated symmetry breaking

We first begin with the introduction of the representation basis of the magnetic order parameters using the local magnetic moments. However, we would like to emphasize that the analysis that we employ here are based on the symmetry of the system. Therefore, the conclusion does not depend on whether the magnetic order parameters involve localized moments or itinerant electrons.

The overall results are summarized in Table 1. In the sector "at T_0" of Table 1, we marked the cases where the magneto-elastic coupling between strain and an irreducible representation at $\vec{Q}$ of the space group is allowed by symmetry. In those cases, we can expect a discontinuous jump of the elastic constants at the magnetic transition at $T = T_0$. $\times$ marks the cases where such magneto-elastic coupling linear in a strain and quadratic in order parameters is forbidden. The sector "at T_c" displays the symmetry of the magnetic state in $T < T_0$ and the possibility of discontinuous change of elastic constants at T_c via a strain-order parameter coupling. As for the direction of the magnetic state, only the saddle point solutions of the Landau free energy quartic in the magnetic order parameters are considered.

As shown in Table 1, neither the Pomeranchuk-type antiferromagnet state with $\vec{Q} = \Gamma$ and nor unit-cell doubling antiferromagnetic state causes discontinuous jumps of C_{66} and C_{44} simultaneously at T_0. Furthermore, there is no case with discontinuous changes of both $C_{11} - C_{12}$ and C_{66} at T_c. To have discontinuity of both elastic constants, the set of point-group operations of the

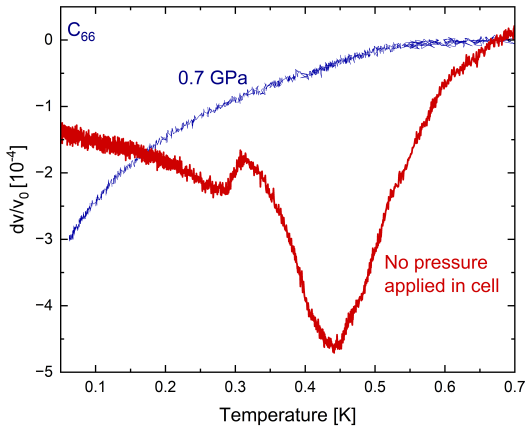

Figure S3. Temperature dependence of the elastic mode C_{66} measured in the pressure cell with and without applied pressure. Measurements under pressure do not show any anomalt that woudl indicate a phase transition.

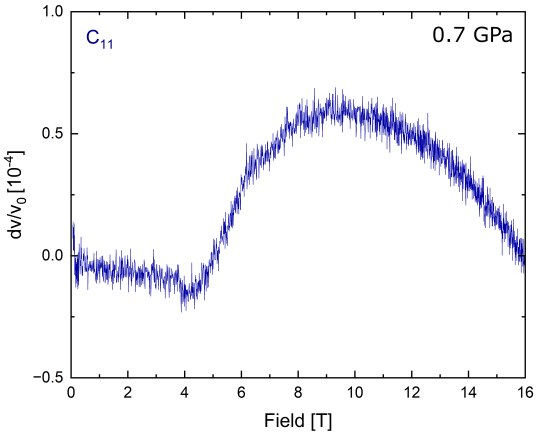

Figure S4. Field dependence of the elastic mode C_{11} under pressure. Signatures related to phase I are absent. However, the transition between the two SC phases remains visible.

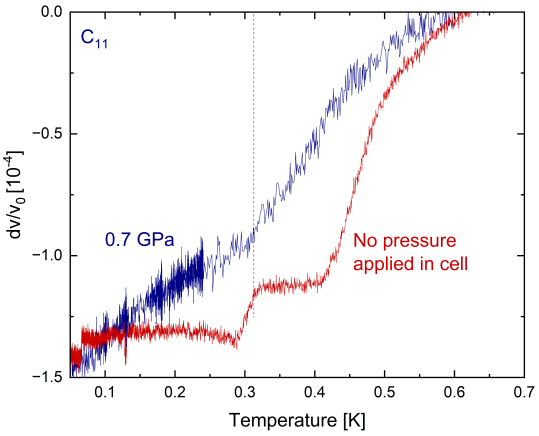

Figure S5. Comparison of the temperature dependence of the C_{11} elastic mode measured under pressure and in ambient conditions. Measurements under pressure do not show any anomaly indicating phase I, but only a weak kink at T_c.

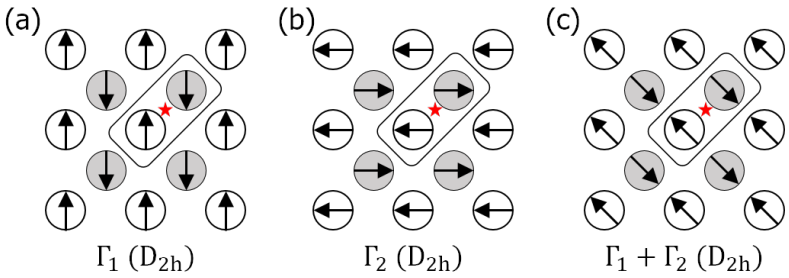

Figure S6. The representation basis of two-components antiferromagnetic orders with $\vec{Q} = \Gamma(0,0,0)$ viewed from the c-axis of the tetragonal lattice. (a) and (b) illustrate the two components, and (c) shows the order parameter along the (m,m) direction in the representation basis. Gray and empty circles represent two distinct Ce sublattices, and arrows depict the in-plane local magnetic moments. Red stars indicate inversion centers, rectangles denote the structural unit cell which coincides with the magnetic unit cell when $\vec{Q} = \Gamma$. The point-group symbol appearing in parentheses in each panel represents the set of the point-group operations preserved in the magnetic phase associated with magnetic order depicted in that panel.

symmetries preserved in the magnetic state should be included in a monoclinic point-group $C_{2h} = \{e, \mathscr{I}, C_{2,001}, m_{001}\}$ where $\mathscr{I}$ is a spatial inversion, $C_{2,001}$ and m_{001} are the rotation along the crystallographic c axis and the reflection against the ab plane, respectively. As for the magnetic states in Table S1 whose remaining symmetry is denoted as C_{2h}, these C_{2h} groups involve rotations along in-plane directions.

We note that two-component superconductivity is not possible in monoclinic and orthorhombic systems. Therefore, if the discontinuous changes of $(C_{11} - C_{12})/2$ and C_{66} are due to the onset of two-component superconductivity, only three cases of Table 1 are compatible: magnetic state (m,m) with $\vec{Q} = M$ and the magnetic states $(m,0,m,0)$ and $(m,0,0,m)$ with $\vec{Q} = X$.

3.1 Basis for antiferromagnetic orders with $\vec{Q}$ at $\Gamma(0,0,0)$ or $Z(0,0,\pi)$

We first want to note that the irreducible representations at the $\Gamma(0,0,0)$ and $Z(0,0,\pi)$ points of the first Brillouin zone match, with identical representation matrices. Thus, from the symmetry point of view, these two points are equivalent, which let us focus just on the case of $\vec{Q} = \Gamma$. There are two irreducible representations without net magnetization over a primitive unit cell. One of them is a one-dimensional irreducible representation, whose representation basis can be characterized by two antiparallel local magnetic moments along the c axis at two Ce sites. As it is one-dimensional, it cannot couple to strains relevant to $C_{11} - C_{12}$ and C_{66} via a magneto-elastic coupling linear in the strain and quadratic in order parameters. Therefore, we neglect this case.

The other irreducible representation is a two-dimensional, or two-component, irreducible representation, whose symmetry properties can be understood by using the in-plane local magnetic moments at two Ce sites. Figures S6(a) and S6(b) illustrate

	At T_0			At T_c			
$\vec{Q}$	C_O (B_{1g})	C_{66} (B_{2g})	C_{44} (E_g)	Direction and Remaining symmetry	C_O (B_{1g})	C_{66} (B_{2g})	C_{44} (E_g)
Γ/Z	✓	✓	×	$(m,0):D_{2h}$	✓	×	×
				$(m,m):D_{2h}$	×	✓	×
M/A	×	✓	×	$(m,0):D_{2h}$	×	✓	×
				$(m,m):D_{2d}$	×	×	×
X/R	✓	×	✓	$(m,0,0,0):C_{2v}$	✓	×	×
				$(m,m,0,0):C_{2h}$	✓	×	✓
				[m] $(m,0,m,0):C_{4v}$ $(m,0,0,m):D_{2d}$	×	×	×
				$(m,m,m,m):C_{2h}$	×	✓	✓

Table 1. Elastic constants that can have discontinuous jumps at the magnetic transition at T_0 and the superconducting transition at T_c. $\vec{Q}$ denotes the ordering vector of magnetic states that emerge at T_0. $C_O = (C_{11} - C_{12})/2$. The first column of the "At T_c" sector shows the direction of the magnetic order in the representation basis introduced in Secs. 3.1–3.3 along with the point-group equivalent to the set of point-group operations of the symmetries preserved in the magnetic state. B_{1g}, B_{2g}, and E_g in parenthesis in the second row represent the symmetry properties of the strains associated with the elastic constants in tetragonal system. ✓ marks the cases where a strain-order parameter coupling linear in a shear strain and quadratic in order parameters deriving the associated transition is allowed by symmetry, which results in a discontinuous jump of the elastic constant. × marks the cases where such strain-order parameter coupling is forbidden by symmetry.

the two components Γ_1 and Γ_2 of the two-dimensional irreducible representation, respectively. The general order parameter is expressed as a linear combination $m_1\Gamma_1 + m_2\Gamma_2$. Such general order parameter can be denoted just simply with the direction (m_1, m_2). $(m,0)$ is just what is shown in Fig. S6(a), while Fig. S6(c) displays the order parameter characterized by the direction (m,m) in the representation basis. The symmetry group of the magnetic phase depends on the direction of the magnetic order. The set of point-group operations of the symmetry group of each magnetic phase is given in Fig. S6. These symmetries are crucial as they decide on the possibility of the discontinuous jumps of an elastic constant at T_c through a magneto-elastic coupling linear in a strain and quadratic in order parameters.

3.2 Basis for the antiferromagnetic orders with $\vec{Q}$ at $M(\pi,\pi,0)$ or $A(\pi,\pi,\pi)$

The M and A points are equivalent in the sense that there is a direct match between their irreducible representations. Thus, we consider only the case of M here. There are two two-dimensional irreducible representations $M^{(1)}$ and $M^{(2)}$, which can be induced by using in-plane local magnetic moments at two distinct Ce sublattices, and one two-dimensional irreducible representations $M^{(3)}$ induced by out-of-plane local magnetic moments at two distinct Ce sublattices. When it comes to the free energy up to quartic order in the order parameters and the magneto-elastic couplings with strains, these three irreducible representations are equivalent. Therefore, we present the representation basis just for $M^{(1)}$ in Fig. S7. The representation basis for $M^{(2)}$ can be obtained by rotating the basis for $M^{(1)}$ by 90°, while the basis for $M^{(3)}$ is derived by replacing the in-plane moments with out-of-plane moments.

Note that all these irreducible representations are mixed in parity under the spatial inversion? due to the non-symmorphic symmetries in the space group 129.

3.3 Basis for the antiferromagnetic orders with $\vec{Q}$ at $X\{(0,\pi,0),(\pi,0,0)\}$ or $R\{(0,\pi,\pi),(\pi,0,\pi)\}$

The X and R points are also equivalent. Thus, we consider only the case of X here. There are two two-dimensional irreducible representations at $X(\pi,0,0)$ point. As these two have no difference in the formal form of the Landau free energy and the magneto-elastic couplings with strain fields, we focus on the case with $\vec{Q} = X(0,\pi,0)$. The relevant two components of the irreducible representation basis are displayed in Fig. S8(a) and S8(b).

Since the high-symmetry points $X(\pi,0,0)$ on the x-axis and $X(0,\pi,0)$ on the y-axis of the Brillouin zone are intertwined through symmetries, we need to consider the order parameters with ordering vector $\vec{Q} = (\pi,0,0)$ and $\vec{Q} = (0,\pi,0)$ together for a complete symmetry analysis. The two additional components with $\vec{Q} = (\pi,0,0)$ are derived by rotating the two components in Figs. S8(a-b) by 90° deg. The resultant bases are illustrated in Figs. S8(c) and S8(d). By denoting each components as X_1, X_2, X_3, and X_4, the general order parameter is written as $m_1X_1 + m_2X_2 + m_3X_3 + m_4X_4$, or just simply by its direction (m_1, m_2, m_3, m_4) in the representation basis. Two representative examples with order parameters characterized by their direction

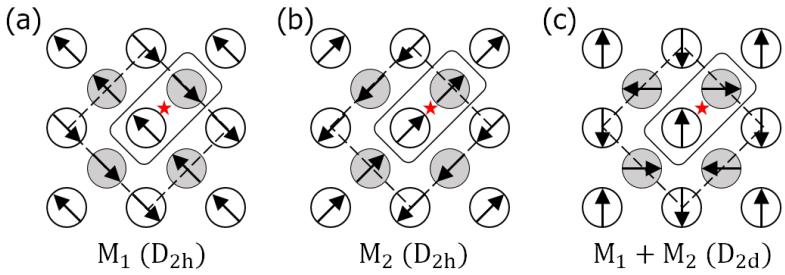

Figure S7. The representation basis of two-component antiferromagnetic orders with $\vec{Q} = M(\pi,\pi,0)$, viewed along the c axis of the tetragonal lattice, is shown. Among the two relevant two-dimensional irreducible representations, $M^{(1)}$ and $M^{(2)}$, only the representation basis transforming according to $M^{(1)}$ is illustrated. (a) and (b) illustrate the two components, and (c) shows the order parameter along the (m,m) direction in the representation basis for $M^{(1)}$. Gray and empty circles represent two distinct Ce sublattices, and arrows depict the in-plane local magnetic moments. Red stars indicate inversion centers, rectangles denote the structural unit cell, and the magnetic unit cell is shown as a diamond with dashed edges. The point-group symbol appearing in parentheses in each panel represents the set of the point-group operations preserved in the magnetic phase associated with magnetic order depicted in that panel.

$(m,0,0,0)$ and $(m,0,m,0)$, are illustrated in Figs. S8(a) and S8(e). The former (latter) is called single-Q (double-Q) phase in literature.

4 Phenomenological analysis of the discontinuity in elastic constants

4.1 Correction to the elastic constant due to order parameter

In the ultrasound measurement, the time for sound to traverse the sample is measured, gives the sound velocity along the propagation direction of the sound. The sound velocity $v_{\vec{k}}$ along the direction $\vec{k}$ is related to the elastic constant C through the relation $C = \rho v^2$, with the density of the crystal ρ. In thermodynamics, elastic constants are defined as the change of stress σ induced by strain ε. Stress is regarded as the conjugate field of the corresponding strain, and thus, it can be obtained by taking the first derivative of the free energy with respect to the strain: $\sigma = \partial F/\partial\varepsilon$. As a result, the elastic constant can be obtained by examining the second derivative of the free energy with respect to the strain: $C = \partial^2 F/\partial\varepsilon^2$. When multiple strains are considered together, the elastic constants are generally obtained by $C_{ij} = \partial^2 F/\partial\varepsilon_i\partial\varepsilon_j$, with i labeling the strains.

When there are other fields ψ_i with $i = 1,2,\cdots$, which typically represent order parameters, besides the strain in the free energy, so that the free energy is a functional $F[\psi_i,\varepsilon]$, the global minimum of the free energy under stress σ is found by solving the saddle-point equations $\partial F[\psi_i,\varepsilon]/\partial\psi_i = 0$ and $\partial F[\psi_i,\varepsilon]/\partial\varepsilon = \sigma$. Denoting the solution of the saddle point at the global minima as $(\psi_i(\sigma),\varepsilon(\sigma))$, the elastic constant is obtained via

$$C = \left.\frac{\partial\sigma}{\partial\varepsilon}\right|_{\sigma=0} = \left[\frac{\partial}{\partial\varepsilon}\left(\left.\frac{\partial F[\psi_i,\varepsilon]}{\partial\varepsilon}\right|_{\psi=\psi(\sigma),\varepsilon=\varepsilon(\sigma)}\right)\right]_{\sigma=0} \tag{1}$$

$$= \left(\frac{\partial^2 F[\psi_i,\varepsilon]}{\partial\varepsilon^2} + \frac{\partial^2 F[\psi_i,\varepsilon]}{\partial\psi_i\partial\varepsilon}\frac{\partial\psi_i(\sigma)}{\partial\varepsilon}\right)_{\sigma=0} \tag{2}$$

$$= \left.\frac{\partial^2 F(\psi_i,\varepsilon)}{\partial\varepsilon^2}\right|_{\psi_i(0),\varepsilon(0)} - \left[\frac{\partial F(\psi_i,\varepsilon)}{\partial\varepsilon\partial\psi_i}\left(\frac{\partial^2 F(\psi_i,\varepsilon)}{\partial\psi_i\partial\psi_j}\right)^{-1}\frac{\partial F(\psi_j,\varepsilon)}{\partial\psi_j\partial\varepsilon}\right]_{\psi(0),\varepsilon(0)}, \tag{3}$$

where we use $\left.\frac{\partial^2 F(\psi,\varepsilon)}{\partial\psi_i\partial_j\psi}\right|_{\psi(\sigma)}\frac{\partial\psi_j(\sigma)}{\partial\varepsilon} + \left.\frac{\partial F(\psi,\varepsilon)}{\partial\psi_i\partial\varepsilon}\right|_{\psi(\sigma)} = 0$ derived from $\frac{\partial}{\partial\varepsilon}\left[\left.\frac{\partial F[\psi_i,\varepsilon]}{\partial\psi_i}\right|_{\psi(\sigma),\varepsilon(\sigma)}\right] = 0$. The first term is just the second-order partial derivative of the free energy, and thus, it is the *bare* elastic constant C_0. Thus, the second term describes the difference due to the presence of the order parameters ψ_i. As the condensation of the order parameter occurs at a lower temperature, we define the change of the elastic constant as

$$\delta C \equiv C_0 - C = \left[\frac{\partial F(\psi_i,\varepsilon)}{\partial\varepsilon\partial\psi_i}\left(\frac{\partial^2 F(\psi_i,\varepsilon)}{\partial\psi_i\partial\psi_j}\right)^{-1}\frac{\partial F(\psi_j,\varepsilon)}{\partial\psi_j\partial\varepsilon}\right]_{\psi(0),\varepsilon(0)}, \tag{4}$$

which will be used to obtain the change of the elastic constants at the transition in the following subsections.

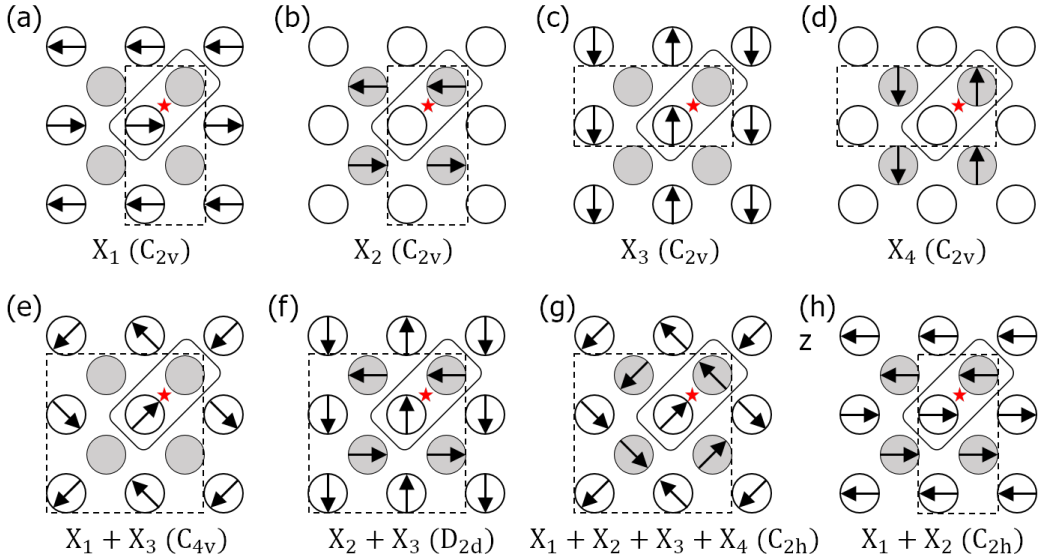

Figure S8. Representation basis of two-component antiferromagnetic orders with $\vec{Q} = X(\pi,0,0)$ or $\vec{Q} = X(0,\pi,0)$, viewed along the c axis of the tetragonal lattice. (a) and (d) illustrate the two basis states with $\vec{Q} = (0,\pi,0)$, while (c) and (d) the remaining two with $\vec{Q} = (\pi,0,0)$. (e-h) show the states obtained by linear combinations of the basis states in (a-d). Gray and open circles represent two distinct Ce sublattices, and arrows depict the in-plane local magnetic moments. Red stars indicate inversion centers, rectangles denote the structural unit cell, and the magnetic unit cell is shown as a diamond with dashed edges. The point-group symbols appearing in parentheses in each panel represents the set of the point-group operations preserved in the magnetic phase associated with magnetic order depicted in that panel.

4.2 The case with $\vec{Q}$ at the $\Gamma(0,0,0)$ and $Z(0,0,\pi)$ point of the first Brillouin zone

As discussed in Sec. 3.1, we consider the antiferromagnetic orders with $\vec{Q} = \Gamma(0,0,0)$ from the phenomenological point of view. Exactly the same conclusion can be drawn for the magnetic ordering with $\vec{Q} = Z(0,0,\pi)$.

As the general magnetic order parameter with $\vec{Q} = \Gamma(0,0,0)$ is written as $M = m_1\Gamma_1 + m_2\Gamma_2$, the Landau free energy should involve two order parameters m_1 and m_2, which correspond to the direction of the general magnetic order parameter in the representation basis. By symmetry consideration, the Landau free energy with symmetry-allowed magneto-elastic couplings is given by

$$F = F_{\rm AFM} + \frac{1}{2}C^{(0)}_{x^2-y^2}\varepsilon^2_{x^2-y^2} + \frac{1}{2}C^{(0)}_{xy}\varepsilon^2_{xy} + F_{\rm me}, \tag{5}$$

$$F_{\rm AFM} = \alpha(m_1^2+m_2^2) + \beta_1(m_1^4+m_2^4) + \beta_2 m_1^2 m_2^2, \tag{6}$$

$$F_{\rm me} = \gamma_{x^2-y^2}\varepsilon_{x^2-y^2}(m_1^2-m_2^2) + 2\gamma_{xy}\varepsilon_{xy}m_1m_2, \tag{7}$$

with $C^{(0)}_{x^2-y^2} = C^{(0)}_{11} - C^{(0)}_{12}$ and $C^{(0)}_{xy} = C^{(0)}_{66}$. The free energy is stable when $2\beta_1+\beta_2 > 0$ and $\beta_1 > 0$. Note that the strains relevant for the elastic constant C_{44}, which transforms according to the irreducible representation E_g of the point-group D_{4h}, do not couple to the magnetic order considered here through the couplings linear in a shear strain and quadratic in the order parameters; moreover, we ignore the coupling to the A_{1g} strains relevant for the elastic constant $C_{11}+C_{12}$ since this is always present. The global minimum of the free energy and the associated discontinuity of the elastic constants $C_{x^2-y^2}$ and C_{xy} are found at points (m_1,m_2) equivalent to either

$$(m_1,m_2) = \sqrt{\frac{-\alpha}{2\beta_1-\beta_{x^2-y^2}}}(1,0), \quad (\varepsilon_{x^2-y^2},\varepsilon_{xy}) = (\frac{\beta_{x^2-y^2}}{2\beta_1-\beta_{x^2-y^2}}\frac{\alpha}{\gamma_{x^2-y^2}},0), \tag{8}$$

$$(m_1,m_2) = \sqrt{\frac{-\alpha}{2\beta_1+\beta_2-\beta_{xy}}}(1,1), \quad (\varepsilon_{x^2-y^2},\varepsilon_{xy}) = (0,\frac{2\beta_{xy}}{2\beta_1+\beta_2-2\beta_{xy}}\frac{\alpha}{\gamma_{xy}}), \tag{9}$$

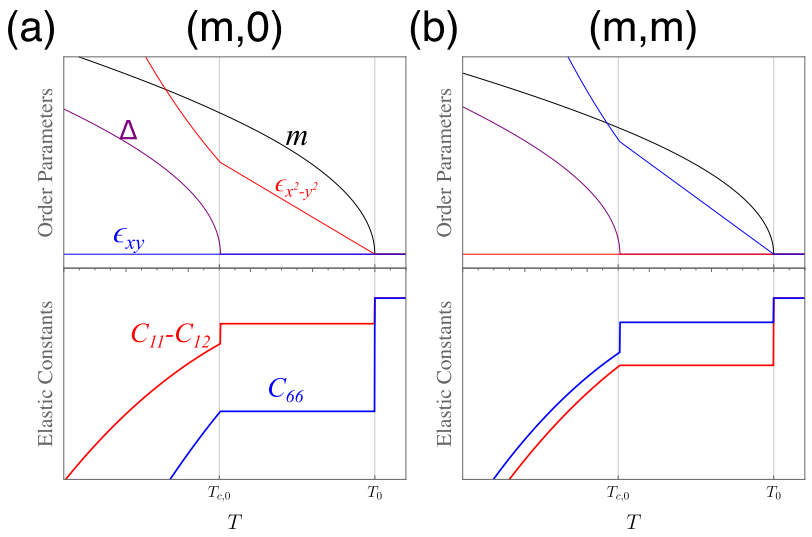

Figure S9. Schematic evolution of the overall magnitude m of the magnetic order parameter with $\vec{Q} = \Gamma$, the superconducting order parameter Δ, and the strains $\varepsilon_{x^2-y^2}$ and ε_{xy} with respect to temperature. At the top of each panel, the direction of the magnetic order in the representation basis is given. For each panel, the parameters of the free energy in Eq. (5) are chosen to stabilize the corresponding magnetic state as the ground state below T_0.

with $\beta_{x^2-y^2} = \gamma^2_{x^2-y^2}/C^{(0)}_{x^2-y^2}$ and $\beta_{xy} = \gamma^2_{xy}/C^{(0)}_{xy}$. The associated discontinuity at the magnetic transition is given by

$$\frac{\delta C_{x^2-y^2}}{C^{(0)}_{x^2-y^2}} = \frac{\beta_{x^2-y^2}}{2\beta_1}, \frac{\delta C_{xy}}{C^{(0)}_{xy}} = \frac{2\beta_{xy}}{-(2\beta_1-\beta_2-2\beta_{x^2-y^2})} \quad \text{, when } (m_1,m_2) = (m,0), \tag{10}$$

$$\frac{\delta C_{x^2-y^2}}{C^{(0)}_{x^2-y^2}} = \frac{2\beta_{x^2-y^2}}{2\beta_1-\beta_2+2\beta_{x^2-y^2}}, \frac{\delta C_{xy}}{C^{(0)}_{xy}} = \frac{2\beta_{xy}}{2\beta_1+\beta_2} \quad \text{, when } (m_1,m_2) = (m,m). \tag{11}$$

As the experimentally observed relative change of the elastic constants is typically less than 10^{-5}, we can assume that both $\beta_{x^2-y^2}$ and β_{xy} are much smaller than β_1 and $2\beta_1+\beta_2$. Given this hierarchy between the parameters, the first solution with either of m_1 and m_2 non-zero is the ground state when $2\beta_1-\beta_2 < 2\beta_{x^2-y^2}-2\beta_{xy}$, which implies $2\beta_1 \lesssim \beta_2$. The second solution corresponds to the case, where the direction of the ground-state order parameter is represented as (m,m) shown in Fig. S6(c). This becomes the ground state when $2\beta_1-\beta_2 > 2(\beta_{x^2-y^2}-\beta_{xy})$.

Figure S9 displays schematics of the order parameters and the relative change of elastic constants. The superconducting order parameter Δ is considered by modifying the free energy Eq. 5 as $F \to F + F_\Delta$ where

$$F_\Delta = (T-T_{c,0})\Delta^2 + \beta_\Delta\Delta^4 + \Delta^2\{\gamma^{(\Delta)}_{x^2-y^2}\varepsilon_{x^2-y^2}(m_1^2-m_2^2) + 2\gamma^{(\Delta)}_{xy}\varepsilon_{xy}m_1m_2\} \tag{12}$$

with the temperature T and the bare superconducting critical temperature $T_{c,0}$. We choose $\gamma^{(\Delta)}_i = 3.5\gamma_i$ to make the effect of the superconducting transition evident for readability; although this is likely exaggerated, it does not qualitatively effect our conclusions.

Note that, although discontinuous jumps of the two elastic constants are expected at the transition at $T = T_0$, regardless of the direction of the ground-state magnetic ordering, both ground states have a different set of symmetries broken at the transition. This is reflected by the strain with finite amplitude after the transition, which means a distortion of the lattice in accordance with the symmetry lowering at the onset of the magnetic ordering. The sets of the point-group operation of the symmetries preserved in the two magnetic states are isomorphic to the point-group D_{2h}. The difference is that the magnetic phase with $(m_1,m_2) \sim (m,0)$ preserves two-fold rotations along the crystallographic a and b axis. In this case, a single-component superconducting order parameter Δ can couple to the strain $\varepsilon_{x^2-y^2}$ associated with $C_{11}-C_{12}$ via the magneto-elastic coupling $g\varepsilon_{x^2-y^2}|\Delta|^2$ where $g \propto m_1^2-m_2^2$. Consequently, a discontinuity of $C_{x^2-y^2} = C_{11}-C_{12}$ can occur at $T = T_c < T_0$. Meanwhile, the magnetic phase with $(m_1,m_2) \sim (m,m)$ has two-fold rotations along the (110) and $(1\bar{1}0)$ directions. Thus, a coupling $g\varepsilon_{xy}|\Delta|^2$ where $g \propto m_1m_2$ is allowed, which leads to a discontinuity of $C_{xy} = C_{66}$ at $T = T_c < T_0$. The schematic behavior of the magnetic order parameters (m_1,m_2), the superconducting order parameter $|\Delta|$, and the associated change of elastic shear constants are shown in Figure S9.

4.3 The case with $\vec{Q}$ at the $M(\pi,\pi,0)$ and $A(\pi,\pi,\pi)$ point of the first Brillouin zone

As discussed in Sec. 3.1, we can focus on the phenomenological theory of a magneto-elastic system with magnetic order transforming according to the irreducible representation $M^{(1)}$ in this case. Including the symmetry-allowed linear-quadratic magneto-elastic coupling between the strain ε and the general magnetic order parameter $M = m_1 M_1^{(1)} + m_2 M_2^{(1)}$, the Landau free energy is given by

$$F = F_{\mathrm{AFM}} + \frac{1}{2} C_{xy}^{(0)} \varepsilon_{xy}^2 + F_{\mathrm{me}}, \tag{13}$$

$$F_{\mathrm{AFM}} = \alpha(m_1^2 + m_2^2) + \beta_1(m_1^4 + m_2^4) + \beta_2 m_1^2 m_2^2, \tag{14}$$

$$F_{\mathrm{me}} = \gamma_{xy}\varepsilon_{xy}(m_1^2 - m_2^2), \tag{15}$$

with $C_{xy}^{(0)} = C_{66}^{(0)}$. Note that the strains relevant for the elastic constants $(C_{11} - C_{12})/2$ and C_{44}, which transform according to the irreducible representations $B_{1\mathrm{g}}$ and E_g of the point-group $D_{4\mathrm{h}}$, respectively, do not couple to the magnetic orders considered here through the a coupling linear in the strain and quadratic in the order parameters.

The saddle-point solutions are found at

$$(m_1, m_2) = \sqrt{\frac{-\alpha}{2\beta_1 - \beta_{xy}}}(1,0), \quad \varepsilon_{xy} = \frac{\beta_{xy}}{2\beta_1 - \beta_{xy}} \frac{\alpha}{\gamma_{xy}}, \tag{16}$$

$$(m_1, m_2) = \sqrt{\frac{-\alpha}{2\beta_1 + \beta_2}}(1,1), \quad \varepsilon_{xy} = 0, \tag{17}$$

with $\beta_{xy} = \gamma_{xy}^2 / C_{xy}^{(0)}$. The associated discontinuity at the magnetic transition is given by

$$\frac{\delta C_{xy}}{C_{xy}^{(0)}} = \frac{\beta_{xy}}{2\beta_1} \quad \text{when } (m_1, m_2) = (m, 0), \tag{18}$$

$$\frac{\delta C_{xy}}{C_{xy}^{(0)}} = \frac{2\beta_{xy}}{2\beta_1 - \beta_2} \quad \text{when } (m_1, m_2) = (m, m). \tag{19}$$

Note that a discontinuous jump of the elastic constant C_{66} at T_0 is expected regardless of the direction of the ground-state magnetic ordering. However, the set of point-group operations of the symmetries preserved in the magnetic state of the second solution, which is characterized by the direction (m,m), is equivalent to the point-group $D_{2\mathrm{d}}$. Four-fold rotoinversions in the point-group $D_{2\mathrm{d}}$ prevent a strain-order parameter coupling quadratic in a single-component superconducting order parameter and linear in one of the strains $\varepsilon_{x^2-y^2}$ and ε_{xy}, and thus no jump is observed at T_c.

In contrast, the magnetic phase described by the first solution has point-group operations isomorphic to $D_{2\mathrm{h}}$ point-group, and a single-component superconducting order parameter can couple to a strain B_{xy} through a coupling linear in the strain: $g\varepsilon_{xy}|\Delta|^2$ with, $g \propto m_1^2 - m_2^2$. Therefore, a discontinuous jump of C_{66} is expected at the superconducting transition at $T = T_c$.

Figure S10 displays the schematics evolution of the order parameters and the relative change of some elastic constants. The superconducting order parameter Δ is considered by adding $(T - T_{c,0})\Delta^2 + \beta_\Delta \Delta^4 + 2\gamma_{xy}^{(\Delta)} \Delta^2 \varepsilon_{xy}(m_1^2 - m_2^2)$, with the temperature T and the bare superconducting critical temperature $T_{c,0}$. $\gamma_i^{(\Delta)} = 5\gamma_i$ is used to make the change at the superconducting transition better visible.

4.4 The case with $\vec{Q}$ at the $X\{(\pi,0,0),(0,\pi,0)\}$ and $R\{(\pi,0,\pi),(0,\pi,\pi)\}$ point of the first Brillouin zone

The Landau free energy of the magneto-elastic system with magnetic order parameter $M = m_1 X_1 + m_2 X_2 + m_3 X_3 + m_4 X_4$ is written as

$$F = F_{\mathrm{AFM}} + \frac{1}{2} C_{x^2-y^2}^{(0)} \varepsilon_{x^2-y^2}^2 + \frac{1}{2} C_{44}^{(0)} (\varepsilon_{xz}^2 + \varepsilon_{yz}^2) + F_{\mathrm{me}}, \tag{20}$$

$$\begin{aligned} F_{\mathrm{AFM}} = {} & \alpha(m_1^2 + m_2^2 + m_3^2 + m_4^2) + \beta_1(m_1^4 + m_2^4 + m_3^4 + m_4^4) \\ & + \beta_2(m_1^2 m_2^2 + m_3^2 m_4^2) + \beta_3(m_1^2 m_3^2 + m_2^2 m_4^2) + \beta_4(m_1^2 m_4^2 + m_2^2 m_3^2), \end{aligned} \tag{21}$$

$$F_{\mathrm{me}} = \gamma_{x^2-y^2}\varepsilon_{x^2-y^2}(m_1^2 + m_2^2 - m_3^2 - m_4^2) + 2\gamma_{44}(\varepsilon_{xz} m_1 m_2 + \varepsilon_{yz} m_3 m_4). \tag{22}$$

with $C_{x^2-y^2}^{(0)} = (C_{11}^{(0)} - C_{12}^{(0)})/2$. Note that the strains ε_{xz} and ε_{yz} relevant for the elastic constant C_{44} are allowed to couple to the magnetic orders in this case. However, a coupling to the strain ε_{xy} relevant to the elastic constant C_{66} is absent. The saddle-point

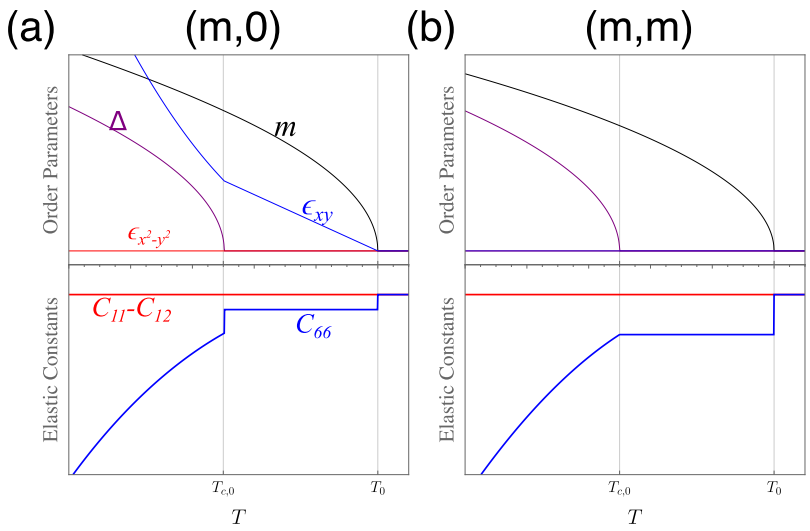

Figure S10. Schematic evolution of the overall magnitude m of the magnetic order parameter with $\vec{Q} = M$, the superconducting order parameter Δ, and the strains $\varepsilon_{x^2-y^2}$ and ε_{xy} with respect to temperature. At the top of each panel, the direction of the magnetic order in the representation basis is given. For each panel, the parameters of the free energy in Eq. (13) are chosen to stabilize the corresponding magnetic state as the ground state below T_0.

equations are given by

$$m_1(\alpha+2\beta_1 m_1^2+\beta_2 m_2^2+\beta_3 m_3^2+\beta_4 m_4^2) = -2\gamma_{x^2-y^2}\varepsilon_{x^2-y^2} m_1 - \gamma_{44}\varepsilon_{xz} m_2, \tag{23}$$

$$m_2(\alpha+2\beta_1 m_2^2+\beta_2 m_1^2+\beta_3 m_4^2+\beta_4 m_3^2) = -2\gamma_{x^2-y^2}\varepsilon_{x^2-y^2} m_2 - \gamma_{44}\varepsilon_{xz} m_1, \tag{24}$$

$$m_3(\alpha+2\beta_1 m_3^2+\beta_2 m_4^2+\beta_3 m_1^2+\beta_4 m_2^2) = 2\gamma_{x^2-y^2}\varepsilon_{x^2-y^2} m_3 - 2\gamma_{44}\varepsilon_{yz} m_4, \tag{25}$$

$$m_4(\alpha+2\beta_1 m_4^2+\beta_2 m_3^2+\beta_3 m_2^2+\beta_4 m_1^2) = 2\gamma_{x^2-y^2}\varepsilon_{x^2-y^2} m_4 - 2\gamma_{44}\varepsilon_{yz} m_3, \tag{26}$$

$$C^{(0)}_{x^2-y^2}\varepsilon_{x^2-y^2} + \gamma_{x^2-y^2}(m_1^2+m_2^2-m_3^2-m_4^2) = 0, \tag{27}$$

$$C^{(0)}_{44}\varepsilon_{xz} + 2\gamma_{44} m_1 m_2 = C^{(0)}_{44}\varepsilon_{yz} + 2\gamma_{44} m_3 m_4 = 0. \tag{28}$$

There are five kinds of solutions which can be represented by the direction of the magnetic order parameter in the represented basis: $(m,0,0,0)$, $(m,0,m,0)$, $(m,0,0,m)$, (m,m,m,m), and $(m,m,0,0)$.

1. The solution $(m,0,0,0)$ comes with

$$m^2 = \frac{-\alpha}{2\beta_1-\beta_{x^2-y^2}},\ (\varepsilon_{x^2-y^2},\varepsilon_{xz},\varepsilon_{yz}) = (\frac{\gamma_{x^2-y^2}}{C_{x^2-y^2}}\frac{\alpha}{2\beta_1-\beta_{x^2-y^2}},0,0), \tag{29}$$

with the free energy $-\alpha^2/(4\beta_1-2\beta_{x^2-y^2})$. This becomes a (local) minima of the free energy when $2\beta_1 < \beta_2$ and $2\beta_1 < \beta_3+2\beta_{x^2-y^2}, \beta_4+2\beta_{x^2-y^2}$. The changes of the elastic constants at the transition are

$$\frac{\delta C_{x^2-y^2}}{C^{(0)}_{x^2-y^2}} = \frac{\beta_{x^2-y^2}}{2\beta_1},\ \frac{\delta C_{xz,xz}}{C^{(0)}_{E_g}} = \frac{2\beta_{44}}{-(2\beta_1-\beta_2)},\ \delta C_{yz,yz} = 0. \tag{30}$$

where $C_{ij} \equiv \partial^2 F/\partial\varepsilon_i\partial\varepsilon_j$. Note that anisotropy between ε_{xz} and ε_{yz} emerges after the transition, which can be understood by the fact that the symmetries preserved in this magnetic state involve point-group operations isomorphic to an orthorhombic point-group C_{2v} with two-fold rotation along the c axis and mirror planes against the tetragonal a and b axis.
In C_{2v} symmetries, the strain $\varepsilon_{x^2-y^2}$ transforms according to the trivial irreducible representation of C_{2v}, and thus, a single-component superconducting order parameter can couple to this strain via a coupling linear in the strain. Consequently, a discontinuous change of $(C_{11}-C_{12})/2$ is expected at T_c, as a consequence of $\varepsilon_{x^2-y^2} \neq 0$ in Eq. (29).

2. The solution $(m,m,0,0)$ comes with

$$m^2 = \frac{-\alpha}{2\beta_1+\beta_2-2\beta_{44}-2\beta_{x^2-y^2}},\ (\varepsilon_{x^2-y^2},\varepsilon_{xz},\varepsilon_{yz}) = \frac{2\alpha(\frac{\gamma_{x^2-y^2}}{C^{(0)}_{x^2-y^2}},\frac{\gamma_{44}}{C^{(0)}_{44}},0)}{2\beta_1+\beta_2-2\beta_{x^2-y^2}-2\beta_{44}}, \tag{31}$$

with the free energy $-\alpha^2/(2\beta_1+\beta_2-2\beta_{44}-2\beta_{x^2-y^2})$. This becomes a (local) minima of the free energy when $2\beta_1+\beta_{44}>|\beta_2-\beta_{44}|$ and $2\beta_1+\beta_2-\beta_3-\beta_4-2\beta_{44}-4\beta_{x^2-y^2}<0$. The changes of the elastic constants at the transition are

$$\frac{\delta C_{x^2-y^2}}{C^{(0)}_{x^2-y^2}} = \frac{2\beta_{x^2-y^2}}{2\beta_1+\beta_2},\ \frac{\delta C_{xz,xz}}{C^{(0)}_{44}} = \frac{\beta_{44}}{2\beta_1+\beta_2},\ \delta C_{yz,yz}=0. \tag{32}$$

Note that the change of the elastic constant C_{44} is anisotropic as it can be known by $|\varepsilon_{xz}|\neq|\varepsilon_{yz}|$. The point-group operations of the preserved symmetries belong to the point-group C_{2h} with a two-fold rotation along the b-axis of tetragonal lattice. In this symmetry, $\varepsilon_{x^2-y^2}$ can couple to a single-component superconducting order parameter via a coupling linear in the strain, but ε_{xy} cannot.

3. The solution $(m,0,m,0)$ comes with

$$m^2 = \frac{-\alpha}{2\beta_1+\beta_3},\ (\varepsilon_{x^2-y^2},\varepsilon_{xz},\varepsilon_{yz}) = (0,0,0), \tag{33}$$

with-free energy $-\alpha^2/(2\beta_1+\beta_3)$. This becomes a (local) minima of the free energy when $|\beta_3|<2\beta_1<\beta_2-\beta_3+\beta_4$. The changes of the elastic constants at the transition are

$$\frac{\delta C_{x^2-y^2}}{C^{(0)}_{B_{1g}}} = \frac{2\beta_{x^2-y^2}}{2\beta_1-\beta_3},\ \frac{\delta C_{xz,xz}}{C^{(0)}_{44}} = \frac{\delta C_{yz,yz}}{C^{(0)}_{44}} = \frac{2\beta_{44}}{-(2\beta_1-\beta_2-\beta_3+\beta_4)}. \tag{34}$$

The set of the point-group operations of the symmetries preserved is isomorphic to the point-group C_{4v}, and thus, a single-component superconducting order parameter cannot couple to the shear strains, such as $\varepsilon_{x^2-y^2}$, ε_{xy}, and $(\varepsilon_{xz},\varepsilon_{yz})$, via a coupling linear in a strain, as it can be known by the fact that all ε's are found to be zero in Eq. (34).

4. The solution $(m,0,0,m)$ can be obtained by exchanging β_3 and β_4 in the expressions for the case of $(m,0,m,0)$:

$$m^2 = \frac{-\alpha}{2\beta_1+\beta_4},\ (\varepsilon_{x^2-y^2},\varepsilon_{xz},\varepsilon_{yz}) = (0,0,0), \tag{35}$$

with free energy $-\alpha^2/(2\beta_1+\beta_4)$. This becomes a (local) minima of the free energy when $|\beta_4|<2\beta_1<\beta_2+\beta_3-\beta_4$. The changes of the elastic constants at the transition are

$$\frac{\delta C_{x^2-y^2}}{C^{(0)}_{B_{1g}}} = \frac{2\beta_{x^2-y^2}}{2\beta_1-\beta_2},\ \frac{\delta C_{xz,xz}}{C^{(0)}_{44}} = \frac{\delta C_{yz,yz}}{C^{(0)}_{44}} = \frac{2\beta_{44}}{-(2\beta_1-\beta_2-\beta_3+\beta_4)}. \tag{36}$$

Though the expressions looks similar to thoes for $(m,0,m,0)$, the resultant symmetry group of the antiferromagnetic state involves point group operations belonging to D_{2d}. However, D_{2d} and C_{4v} are not distinguishable when it comes to the even-parity basis functions relevant to the symmetry of the strain fields; if two even functions belong to the same irreducible irrep in C_{4v}, they belong to the same irrep in D_{2d} as well.

5. The solution (m,m,m,m) comes with

$$m^2 = \frac{-\alpha}{2\beta_1+\beta_2+\beta_3+\beta_4-2\beta_{44}},\ (\varepsilon_{x^2-y^2},\varepsilon_{xz},\varepsilon_{yz}) = \frac{2\gamma_{44}\alpha(0,1,1)}{C^{(0)}_{44}(2\beta_1+\beta_2+\beta_3+\beta_4-2\beta_{44})}, \tag{37}$$

with free-energy $-2\alpha^2/(2\beta_1+\beta_2+\beta_3+\beta_4-2\beta_{44})$. This becomes a (local) minima of the free energy when $2\beta_1+\beta_2>|\beta_2+\beta_4|$ and $2\beta_1-\beta_2+2\beta_{44}>|\beta_3-\beta_4|$. The changes of the elastic constants at the transition are

$$\frac{\delta C_{x^2-y^2}}{C^{(0)}_{x^2-y^2}} = \frac{2\beta_{x^2-y^2}}{2\beta_1+\beta_2-\beta_3-\beta_4},\ \frac{\delta C_{44}}{C^{(0)}_{44}} = \frac{2(2\beta_1+\beta_2)\beta_{44}}{(2\beta_1+\beta_2)^2-(\beta_3+\beta_4)^2}. \tag{38}$$

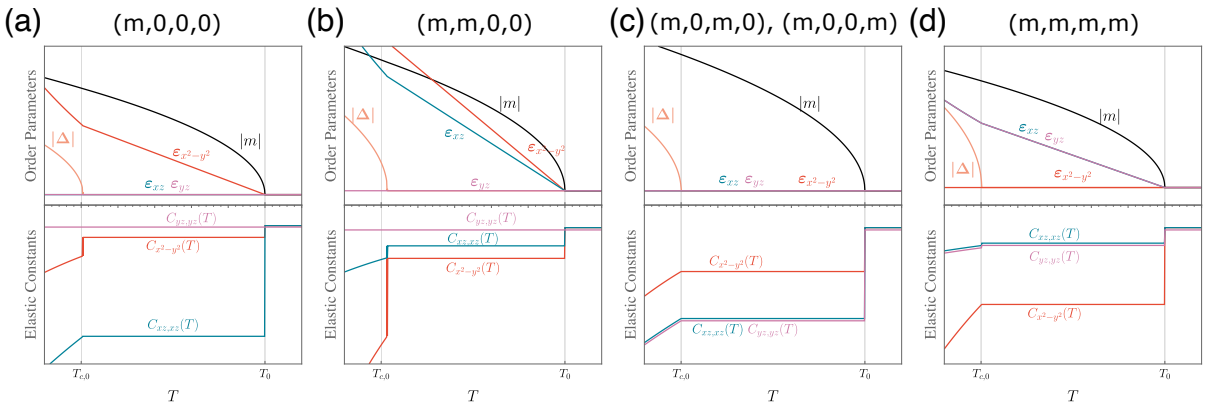

Figure S11. Schematic evolution of the overall magnitude m of the magnetic order parameter with $\vec{Q} = X$, the superconducting order parameter Δ, and the strains ($\varepsilon_{x^2-y^2}$, ε_{xz}, ε_{yz}) with respect to temperature. At the top of each panel, the direction of the magnetic order in the representation basis is given. For each panel, the parameters of the free energy in Eq. (20) are chosen to stabilize the corresponding magnetic state as the ground state below T_0.

The point-group operations of the preserved symmetries belong to the point-group C_{2h} with a two-fold rotation along the (110) direction of the tetragonal lattice. In this symmetry group, the strain ε_{xy} associated with the elastic constant C_{66} transforms trivially, and, thus, it can couple to a single-component superconducting order parameter through a coupling $g\varepsilon_{xy}|\Delta|^2$ with $g \propto m_1 m_2 m_3 m_4$. ε_{xy} transforms non-trivially in C_{2h}, and, thus, it cannot couple to the superconducting order parameter.

5 $\vec{Q}$ off High-symmetry points

As we argued in the main text, the antiferromagnetic ordering occurring at T_0 should involve an ordering vector $\vec{Q}$ on the high-symmetry lines $Y(k_x,\pi,0)$ and $T(k_x,\pi,\pi)$, in the high-symmetry plane $F(k_x,\pi,k_z)$, or at a general point inside the first Brillouin zone to explain the ultrasound measurements. As for symmetry-allowed discontinuities of the elastic constants at T_0 for other ordering vectors on the high-symmetry lines and planes in Brillouin zone of tetragonal systems, see Table 2.

The number of magnetic order parameters with $\vec{Q}$ on the high-symmetry plane $F(k_x,\pi,\pi)$ is 16, while it is 8 for $\vec{Q}$ on the high-symmetry lines $Y(u,\pi,0)$ and $T(u,\pi,\pi)$. For simplicity, we present the phenomenological analysis for the case with $\vec{Q}$ on the line Y. As mentioned, the space-group irreducible representation at $\vec{Q}$ on the line involves 8 components and the Landau free energy is given by

$$F = F_{\mathrm{AFM}} + \frac{1}{2}C^{(0)}_{x^2-y^2}\varepsilon^2_{x^2-y^2} + \frac{1}{2}C^{(0)}_{xy}\varepsilon^2_{xy} + \frac{1}{2}C^{(0)}_{44}(\varepsilon^2_{xz}+\varepsilon^2_{yz}) + F_{\mathrm{me}}, \tag{39}$$

$$F_{\mathrm{AFM}} = \alpha I_{A_{1g}} + \beta_1 I^2_{A_{1g}} + \beta_2 I^2_{B_{1g}} + \beta_3 I^2_{B_{2g}} + \beta_4 I^2_{A_{2u}} + \beta_5 I^2_{B_{2u}} + \beta_6 (I^2_{E_g,yz} + I^2_{E_g,xz}), \tag{40}$$

$$F_{\mathrm{me}} = \gamma_{x^2-y^2}\varepsilon_{x^2-y^2} I_{B_{1g}} + \gamma_{xy}\varepsilon_{xy} I_{B_{2g}} + \gamma_{44}\{\varepsilon_{xz} I_{E_g,xz} + \varepsilon_{yz} I_{E_g,yz}\}, \tag{41}$$

with

$$I_{A_{1g}} = m_1^2 + m_2^2 + m_3^2 + m_4^2 + m_5^2 + m_6^2 + m_7^2 + m_8^2, \tag{42}$$

$$I_{B_{1g}} = m_1^2 + m_2^2 + m_3^2 + m_4^2 - m_5^2 - m_6^2 - m_7^2 - m_8^2, \tag{43}$$

$$I_{B_{2g}} = m_1 m_2 + m_3 m_4 - m_5 m_6 - m_7 m_8, \tag{44}$$

$$I_{A_{2g}} = m_1 m_2 + m_3 m_4 + m_5 m_6 + m_7 m_8, \tag{45}$$

$$I_{A_{2u}} = m_1 m_3 - m_2 m_4 + m_5 m_7 - m_6 m_8, \tag{46}$$

$$I_{B_{2u}} = m_1 m_3 - m_2 m_4 - m_5 m_7 + m_6 m_8, \tag{47}$$

$$I_{E_g,xz} = m_1^2 - m_2^2 + m_3^2 - m_4^2 \to m_1^2 - m_2^2 - m_3^2 + m_4^2, \tag{48}$$

$$I_{E_g,yz} = m_5^2 - m_6^2 + m_7^2 - m_8^2 \to m_5^2 - m_6^2 - m_7^2 + m_8^2, \tag{49}$$

where all m_i are real order parameters. $m_{1,\cdots,4}$ describe order parameters oscillating like $\cos(k_x x + \pi y)$, and $\sin(k_x x + \pi y)$ while $m_{5,\cdots,8}$ are derived from $\cos(\pi x + k_y y)$ and $\sin(\pi x + k_y y)$. Among the quartic terms in F_{AFM}, $I^2_{A_{2g}}$ does not appear as it can be

$\vec{Q}$	$C_O\,(B_{1g})$	$C_{66}\,(B_{2g})$	$C_{44}\,(E_g)$
$\Delta(0,u,0)/U(0,u,\pi)$	✓	×	×
$\Sigma(u,u,0)/S(u,u,\pi)$	×	✓	×
$Y(u,\pi,0)/T(u,\pi,\pi)$	✓	✓	✓
$\Lambda(0,0,u)$	✓	✓	×
$W(0,\pi,u)$	✓	×	✓
$V(\pi,\pi,u)$	×	✓	×
$D(u,v,0)/E(u,v,\pi)$	✓	✓	×
$F(u,\pi,v)$	✓	✓	✓
$C(u,u,v)$	×	✓	✓
$B(0,u,v)$	✓	×	✓
$GP(u,v,w)$	✓	✓	✓

Table 2. Elastic constants that can exhibit a discontinuous change at T_0 associated with the ordering vector $\vec{Q}$. The first column shows the ordering vector $\vec{Q}$ emerging at T_0. $C_O = (C_{11} - C_{12})/2$. The other three columns display whether a discontinuous change at T_0 of the associated elastic strain is permitted by symmetry.

expressed as a linear combination of the other six I^2s. Though obtaining a complete set of solutions of the saddle point equations with twelve variables is impractical, but it is evident that a solution $m_1 = m_2 = m_3 = m_4 = m_a$ and $m_5 = m_6 = m_7 = m_8 = 0$ would result in a discontinuous jump of $C_{11} - C_{12}$ and C_{66} at T_0 with finite $\varepsilon_{x^2-y^2}$ and ε_{xy} below the transition temperature. Furthermore, $C_{xz,xz}$ also exhibits a jump at T_0 without the condensation of ε_{xz} and ε_{yz}, while $C_{yz,yz}$ does not exhibit a discontinuity at T_0.

Indeed, $m_1 = m_2 = m_{a1}$, $m_3 = m_4 = m_{a2}$, and $m_5 = m_6 = m_7 = m_8 = 0$ is expected to occur as the ground-state solution of the Landau free energy when $\beta_2, \beta_3 < 0$ and the other $\beta_{4,5,6}$ are small and positive, so that it is energetically favored to keep $I_{B_{1g}}, I_{B_{2g}} \neq 0$ while $I_{A_{2u}} = I_{B_{2u}} = I_{E_g,xz} = I_{E_g,yz} = 0$. The degeneracy of the states characterized by the same $m_{a,1}^2 + m_{a,2}^2$ is not lifted in the current $\mathcal{O}(m^4)$ expansion of the free energy, and thus let us focus on the cases with $m_1 = m_2 = m_3 = m_4 = m_a$ and $m_5 = m_6 = m_7 = m_8 = m_b$.

In Fig. S12, we compare two ground states of the Landau free energy: (i) $m_a \neq 0$ and $m_b = 0$ and (ii) $m_a = m_b$. Fig. S12(a) displays the case with $m_b = 0$, which is obtained when $4\beta_2 + \beta_3 < 0$ and $\beta_1 > |4\beta_2 + \beta_3|$. Note that $C_{xz,xz}$ and $C_{yz,yz}$ become different below T_0, which are identical to C_{44} above T_0. Despite of the discontinuity in $C_{xz,xz}$ or $C_{yz,yz}$, both shear strains ε_{xz} and ε_{yz} are not finite. Thus, any further discontinuous jump of $C_{xz,xz}$ or $C_{yz,yz}$ is not expected at the superconducting transition. On the other hand, the jumps of the two elastic constants $C_{x^2-y^2}$ and C_{xy} are accompanied by the condensation of $\varepsilon_{x^2-y^2}$ and ε_{xy}. Therefore, additional discontinuities of two elastic constants are expected at the superconducting transition T_c, which is consistent with the result from the ultrasound measurement.

When $4\beta_2 + \beta_3 > 0$ and $\beta_1 > |4\beta_2 + \beta_3|$, the magnetic state with $m_a = m_b$ has a lower free energy than the case with $m_b = 0$. In this case, four shear elastic constants $C_{x^2-y^2}$, C_{xy}, and $C_{xz} = C_{yz}$ are permitted to exhibit a discontinuous jump. However, no shear strain condense: $\varepsilon_{xz} = \varepsilon_{yz} = \varepsilon_{x^2-y^2} = \varepsilon_{xy} = 0$. Therefore, no further discontinuity at the superconducting transition via a strain-order parameter coupling linear in the strain field and quadratic in the superconducting order parameter is expected for all strain channels.

We want to remark that the eigenvalues of the symmetry $\{C_{2y}|0\frac{1}{2}0\}$ of the space group 129 are all complex, which means any real linear combination of the ordering vector is not an eigenvector of the symmetry $\{C_{2y}|0\frac{1}{2}0\}$. Therefore, $\{C_{2y}|0\frac{1}{2}0\}$ is broken in below T_0, which makes the uniform and the staggered superconducting pairings not distinguishable in the strict symmetry sense. However, this does not directly imply a contradiction to the parity-switch scenario for the first-order transition in the superconducting phase. To be specific, the coupling $\mathrm{Re}[\Delta_u^* \Delta_s I_{A_{2u}}]$ which is linear in the uniform superconducting order parameter Δ_u, the staggered superconducting order parameter Δ_s, and quadratic in the incommensurate magnetic order parameter is not effective as long as $I_{A_{2u}} = 0$. Furthermore, the coupling, which is linear in all these three order parameters is forbidden in the normal phase due to the momentum conservation, and it is permitted only in the magnetic phase below T_0. Considering the small magnetic moment $m < 0.2\mu_B$ in $T < T_0$ estimated from the inelastic neutron scattering results TChen2024Expt as well as the adjacency of T_c and T_0, this emergent coupling linear in all three order parameters can be thought of to be not significant. As a result, the low-field and the high-field superconducting states in out-of-plane magnetic fields are still characterized by a

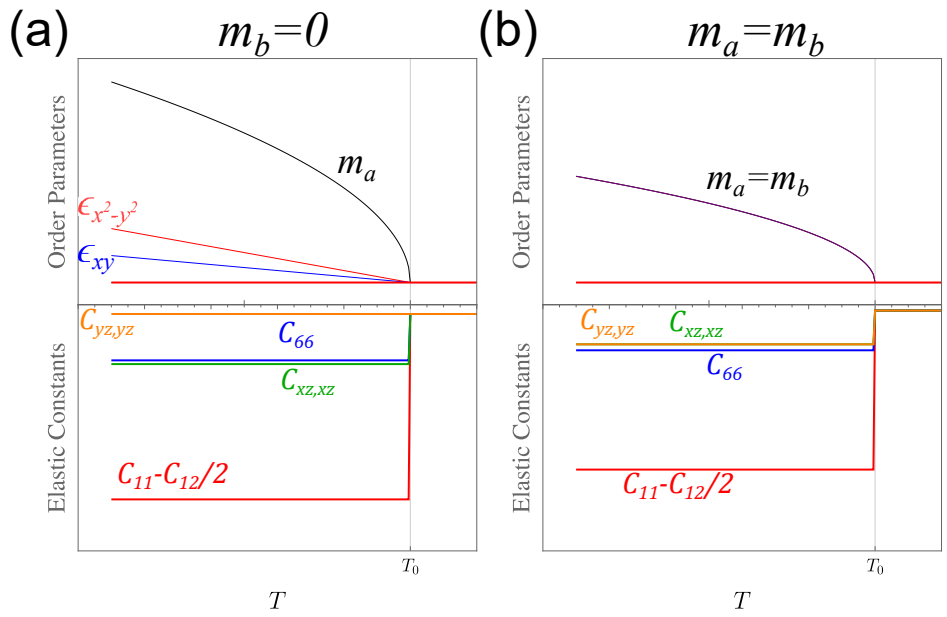

Figure S12. Schematic evolution of the magnitudes of magnetic order parameters m_a and m_b with $\vec{Q} = Y$ and strains ($\varepsilon_{x^2-y^2}$, ε_{xy}, ε_{xz}, ε_{yz}) with respect to temperature. At the top of each panel, the direction of the magnetic order in the representation basis is stated. For each panel, the parameters of the free energy in Eq. (20) are chosen to stabilize the corresponding magnetic state as the ground state below T_0. The bottom of each panel displays the elastic constants.

uniform and a staggered superconducting paring with negligible hybridization.

References

1. Khim, S. *et al.* Field-induced transition within the superconducting state of $CeRh_2As_2$. *Science* **373**, 1012–1016, DOI: 10.1126/science.abe7518 (2021).
2. Khanenko, P. *et al.* Phase diagram of $CeRh_2As_2$ for out-of-plane magnetic field. *Phys. Rev. B* **112**, L060501, DOI: 10.1103/gt54-tvc2 (2025).
3. Pfeiffer, M. *et al.* Pressure-Tuned Quantum Criticality in the Locally Noncentrosymmetric Superconductor $CeRh_2As_2$. *Phys. Rev. Lett.* **133**, 126506, DOI: 10.1103/PhysRevLett.133.126506 (2024).